Degree Day

Hazard Explorer: Technical Methodology

Hazard Data Methodology — Abbreviated • v1.0 • 2026-03-24

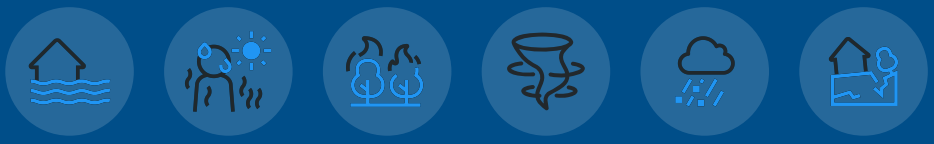

Prepared by D.J. Rasmussen, PhD • Degree Day, LLC
info@degreeday.org • www.degreeday.org

Contents

1 Overview

Intended Use: First-Stage Hazard Screening

The Hazard Explorer is designed as **Step 1** in a structured natural hazards risk management workflow. Its purpose is to identify assets warranting further investigation—not to replace site-specific engineering assessment. By casting a wide net across 18 hazard layers at global scale, it enables rapid triage of large portfolios: surfacing high-exposure assets that merit deeper study while helping demonstrate that lower-scoring assets may be lower priority for immediate follow-up.

Results should be interpreted accordingly. A high score flags a location for follow-on assessment; it is not a loss estimate, engineering finding, or regulatory determination. A low score provides screening-level assurance that hazard exposure does not appear elevated relative to global baselines, given the resolution and methods described herein. Assets flagged by the Hazard Explorer should be prioritized for site-specific study by qualified engineers or hazard specialists before investment or design decisions are made.

The Hazard Explorer provides a consistent framework for assessing the exposure of assets worldwide to both climate-related and geological hazards. Included hazards span flooding, extreme heat, drought, wildfire, extreme winds, hail, earthquakes, landslides, and land subsidence. Rather than developing all datasets from scratch, the methodology curates and integrates dozens of peer-reviewed, globally recognized datasets to ensure that information is scientifically grounded and traceable to recognized source datasets. These data sources include historical weather observations, reanalysis datasets, land cover and elevation data, and specialized models for hazards such as flooding and drought. Data are typically represented on global grids, in some cases down to 90 m resolution for flood inundation.

Each hazard layer is scored on a 1–10 scale with accompanying hazard categories. Table 1 summarizes the hazard metrics presented in the Hazard Explorer, including the physical quantity, statistical basis, units, spatial resolution, and data source for each layer.

Table 1: Summary of hazard metrics in the Hazard Explorer.

Hazard Layer	Metric	Units	Resolution	Source
Wildfire	Annual burn probability (indicative outside U.S. training domain)	%/yr	10″ (∼300 m)	Multi-source; Proprietary
Extreme Heat	Annual max. temperature, 10-yr return level	°C	30″ (∼1 km)	Multi-source; Proprietary
Human Heat Stress	Annual max. wet-bulb temperature, 10-yr return level	°C	30″ (∼1 km)	Multi-source; Proprietary
Human Cold Stress	Annual min. temperature, 10-yr return level	°C	30″ (∼1 km)	Multi-source; Proprietary
Snowfall Intensity	Mean annual max. 1-day snowfall (SWE proxy)	m SWE	∼10 km	Reanalysis
Drought	Composite drought hazard score	Index	Basin	Proprietary
Riverine Flood	Flood depth, multiple return periods	m	3″ (∼90 m)	Multi-source
Coastal Flood	Flood depth, 100-yr return period	m	1″ (∼30 m)	Multi-source
Coastal Exposure	Coastal Exposure Index	Index	1–30 m	Multi-source; Proprietary
Surface Water Flooding	1-hour rainfall depth, 50-yr return level	mm	30″ (∼1 km)	Proprietary
Extreme Wind	3-s wind gust, 1,000-yr return level	km/h	30″ (∼1 km)	Multi-source; Proprietary
Lightning	Annual thunder hours	hrs/yr	∼5 km	Satellite-based
Large Hail	Annual prob. of large hail day (>5 cm)	%/yr	∼31 km	Reanalysis-based
Tornado (U.S.)	Annual prob. of EF2+ tornado	%/yr	∼40 km	Observational
Derecho (U.S.)	Annualized derecho-footprint frequency	yr^{-1}	∼4 km	Observational

Continued on next page

Table 1 continued

Hazard Layer	Metric	Units	Resolution	Source
Earthquake	PGA, 475-yr return period (rock site)	g	∼11 km	Multi-source mosaic
Land Subsidence	Land subsidence rate	mm/yr	30″ (∼1 km)	Physics-informed ML model
Landslide (U.S.)	Susceptibility score	Index	3″ (∼90 m)	USGS
Landslide (Global)	Susceptibility score	Index	3″ (∼90 m)	Published global model
Heating Demand	Annual HDD (base 18.3 °C)	°C-day	30″ (∼1 km)	Multi-source; Proprietary
Cooling Demand	Annual CDD (base 18.3 °C)	°C-day	30″ (∼1 km)	Multi-source; Proprietary

Table 2 describes the practical relevance of each metric and the rationale for the statistical basis or return period chosen.

Table 2: Metric relevance and rationale.

Hazard Layer	Relevance
Wildfire	In the U.S. training domain, annual burn probability quantifies the likelihood that a location experiences wildfire in any given year, informing land-use planning, insurance underwriting, and defensible-space requirements. Outside the U.S. training domain, values are indicative of fire-prone conditions rather than calibrated burn probability estimates.
Extreme Heat	The 10-year return level of annual maximum temperature captures rare but realistic hot extremes that stress infrastructure (pavement buckling, transformer failures, power-grid strain) and affect outdoor worker safety and productivity.
Human Heat Stress	Wet-bulb temperature integrates heat and humidity, reflecting physiological heat-stress limits more accurately than air temperature alone. A 10-year return level identifies locations where dangerous heat-stress episodes affect outdoor worker safety and productivity.
Human Cold Stress	The 10-year return level of annual minimum temperature captures cold extremes that drive pipe bursting, heating-demand spikes, and hypothermia risk. This return period is relevant for outdoor worker safety and mechanical-system design.
Snowfall Intensity	Mean annual maximum 1-day SWE accumulation (a proxy for snowfall intensity) captures the magnitude of the heaviest single-day snow accumulation in a typical year, relevant for structural roof loading, transportation disruption, and emergency planning.
Drought	A composite drought hazard score integrates meteorological, hydrological, and agricultural drought dimensions into a single index, supporting water-supply planning and supply-chain resilience analysis.
Riverine Flood	Flood depth at the asset location directly quantifies inundation severity, making it well suited for screening property exposure and prioritizing sites for detailed hydraulic study. Multiple return periods enable screening at different probability levels.
Coastal Flood	Flood depth at the 100-year return period quantifies inundation severity from combined storm surge, tidal, and sea level forcing, supporting coastal property exposure screening and site prioritization for detailed hydraulic assessment.

Continued on next page

Table 2 continued

Hazard Layer	Relevance
Coastal Exposure	Identifies land areas whose elevation falls below hypothetical extreme coastal water levels, supporting screening of exposure to sea-level rise and other coastal water-level hazards, including storm surge, high tides, wave overtopping, tsunamis, and seiches, for coastal portfolios, infrastructure planning, and site prioritization.
Surface Water Flooding	The 50-year 1-hour rainfall depth captures the short-duration, high-intensity precipitation events most likely to overwhelm urban drainage systems and cause surface water flooding.
Extreme Wind	The 3-second gust is the standard metric for structural wind loading in building codes worldwide. The 1 000-year return period aligns with design standards for critical and essential facilities.
Lightning	Annual thunder hours indicate the frequency of thunderstorm activity, relevant for designing electrical-system protection, assessing outdoor-activity safety, and evaluating wildfire ignition risk from lightning strikes.
Large Hail	Hailstones exceeding 5 cm can cause significant damage to roofs, facades, vehicles, solar panels, and crops. The annual probability of a large-hail day informs material selection, insurance pricing, and maintenance planning.
Tornado (U.S.)	EF2+ tornadoes generate winds exceeding 180 km/h, capable of significant structural damage. The annual probability informs safe-room requirements, shelter planning, and insurance risk. Coverage is limited to the contiguous United States.
Derecho (U.S.)	Derechos are long-lived, widespread windstorms produced by organized convective systems. The annualized footprint frequency quantifies how often a location is affected by derecho-force winds, informing infrastructure resilience, utility planning, and insurance risk. Coverage is limited to the United States east of the Rocky Mountains.
Earthquake	Peak ground acceleration on rock is the standard seismic-hazard metric used in building codes worldwide. The 475-year return period corresponds to a 10 % probability of exceedance in 50 years, the most widely adopted seismic design level.
Land Subsidence	Gradual ground subsidence damages foundations, buried pipelines, roads, aviation runways, and rail infrastructure over time. The annual rate indicates long-term structural and maintenance risk.
Landslide (U.S.)	A susceptibility score reflects terrain vulnerability to landslides based on slope, geology, soil properties, and land cover, supporting development siting and slope-stability screening.
Landslide (Global)	Provides a conceptually similar screening indicator of landslide-prone terrain outside the United States, enabling broad portfolio screening with global coverage. Note that the global and U.S. layers use different underlying methodologies and are not directly comparable.
Heating Demand	Heating degree days quantify cumulative cold exposure that drives space-heating energy consumption. Higher values indicate greater heating costs, fuel demand, and mechanical-system sizing requirements.
Cooling Demand	Cooling degree days quantify cumulative warm exposure that drives space-cooling energy consumption. Higher values indicate greater cooling costs, peak electricity demand, and refrigeration infrastructure needs.

For each hazard, notable advantages and limitations are summarized in the sections below. Because appropriate use cases vary widely, expert judgment is required to interpret results in the context of a specific application. General considerations and limitations applicable to all layers are provided in Section 4.

2 Hazards

2.1 Flooding

Flood hazard is assessed from both inland and coastal sources. Inland flooding encompasses riverine (fluvial) and surface water (pluvial) mechanisms, while coastal flooding captures storm surge, astronomical tides, and mean sea level variability. Each source is evaluated separately due to distinct physical drivers, modeling approaches, and associated uncertainties. The combined flood picture for any given asset should consider all three sources alongside site-specific factors such as drainage infrastructure, flood defenses, and local terrain.

A Note on Elevation Data. Elevation data is the single most influential input to any flood hazard model. Vertical errors in the underlying terrain surface propagate directly into flood depth and inundation extent estimates—a 0.5 m elevation bias in flat coastal terrain can shift the modeled floodplain boundary by hundreds of metres.

Where available, airborne lidar surveys provide sub-decimetre vertical accuracy and are the preferred elevation source. However, lidar coverage remains limited to portions of North America, Western Europe, Oceania, and selected urban areas elsewhere. In regions without lidar, satellite-derived digital elevation models are used. These products are constructed from radar or optical stereo imagery and typically achieve vertical accuracies of 1–3 m (root mean square error) in open, low-slope terrain, but performance degrades in dense urban areas (where radar returns from rooftops and structures inflate apparent ground elevation), heavily forested regions (where canopy returns mask the true ground surface), and steep or complex topography (where shadow and layover effects introduce systematic biases).

For coastal applications, a specialized coastal digital terrain model is used that corrects satellite-derived elevations using spaceborne lidar altimetry. This correction substantially improves inundation mapping in low-lying coastal zones, but residual errors in individual grid cells can still be significant in challenging terrain.

Practical implication: Flood hazard results in regions relying on satellite-derived elevation should be interpreted as screening-level assessments. Where elevation uncertainty is a concern for a specific asset, a ground-level survey or local lidar acquisition is recommended before making investment or engineering decisions.

2.1.1 Inland Flooding

Inland flooding is assessed by analyzing its two primary drivers separately: riverine overflow and surface water accumulation.

Riverine Flood. Riverine flooding occurs when rivers, streams, or other natural channels overflow their banks due to sustained or intense rainfall, snowmelt, or a combination of both. The assessment uses a physically-based modeling chain comprising three stages:

1. **Meteorological forcing.** Multi-decadal reanalysis precipitation and temperature fields are used to drive the hydrological model, providing spatially and temporally consistent rainfall and snowmelt inputs across all major river basins.
2. **Hydrological modeling.** A distributed rainfall-runoff model converts meteorological inputs into river discharge estimates at each stream reach, accounting for soil moisture, evapotranspiration, snowpack dynamics, and upstream routing.
3. **Hydraulic modeling.** A 2D shallow-water solver propagates flood flows across the terrain surface at ∼90 m resolution, producing spatially explicit flood depth and extent maps for multiple return periods (e.g. 20, 50, 100, 200, and 500 years).

Validation. Modeled flood extents have been compared against satellite-observed flood footprints from major historical events across multiple continents and climate zones. Published evaluations show better agreement in wide floodplains and alluvial valleys than in narrow, steep-sided valleys or urban areas where sub-grid-scale flow paths (e.g. culverts, underpasses) are not resolved. Modeled return-period discharges have been validated against long-record gauge stations, with results most reliable in mid-latitude catchments above the minimum upstream area threshold.

Strengths: Globally consistent methodology applied uniformly across all river basins; physically-based modeling chain captures the causal pathway from rainfall through runoff to inundation; multiple return periods enable risk-based screening at different probability levels; resolution (∼90 m) is sufficient to identify floodplain exposure for most commercial and industrial assets.
Limitations: Flood defenses (levees, floodwalls, retention basins) are not represented; all results reflect *undefended* flood hazard (see Section 2.1.3 for defense overlay data). The hydraulic model is not locally calibrated; channel geometry is derived from the DEM rather than surveyed cross-sections. Smaller headwater streams below a minimum upstream drainage area (∼50 km^2) are excluded; flash flooding in small catchments is not captured. Urban

microtopography (buildings, walls, raised infrastructure) is not resolved at 90 m grid spacing. Compound flooding (simultaneous riverine and coastal forcing) is not modeled.

Surface Water Flooding. Surface water (pluvial) flooding occurs when rainfall intensity exceeds local infiltration and drainage capacity, causing water to pond on impervious surfaces or accumulate in topographic depressions. Unlike riverine flooding, surface water flooding is driven by short-duration, high-intensity rainfall events—often lasting minutes to a few hours—and can occur far from any river channel.

Because it is not feasible to simulate drainage networks, urban runoff routing, and local ponding processes at global scale, this hazard is screened using the frequency and magnitude of extreme short-duration rainfall as a proxy for the meteorological conditions most likely to produce surface water flooding.

The extreme rainfall statistics are developed through a multi-step process:

1. **Gauge observations.** Quality-controlled hourly rain gauge records are collected from national meteorological networks. Extreme value distributions are fitted to annual maxima at each station to estimate rainfall intensities at standard return periods (e.g. 10, 25, 50, 100 years).
2. **Convection-permitting simulations.** High-resolution (∼3 km) numerical weather simulations that explicitly resolve deep convection are used to supplement gauge coverage in data-sparse regions and to capture the spatial structure of extreme rainfall fields.
3. **Spatial regionalization.** Station-based and simulated extreme rainfall statistics are combined using physics-informed machine learning regression with environmental predictors (elevation, latitude, distance to coast, mean annual precipitation, land cover) to produce gridded intensity–duration–frequency (IDF) estimates at 30″ (∼1 km) resolution.

Validation. Gridded extreme rainfall estimates have been evaluated against withheld gauge stations using a leave-one-out cross-validation framework. Results are most reliable in gauge-dense regions (North America, Europe, East Asia) and carry greater uncertainty in gauge-sparse regions (Sub-Saharan Africa, Central Asia, parts of South America) where the model relies more heavily on environmental predictors and simulated fields. Broad spatial patterns—wet versus dry regions, orographic enhancement, coastal effects—are generally reproduced at the 1 km scale.

Strengths: Captures the meteorological driver of surface water flooding (extreme short-duration rainfall) at high spatial resolution; convection-permitting simulations provide physically realistic rainfall fields in regions where gauge networks are sparse; IDF-based framework produces results directly comparable to engineering design standards.
Limitations: Results represent extreme rainfall hazard as a proxy; they do not simulate runoff, drainage system performance, or flood depth directly. Two locations with identical rainfall hazard may experience very different flood outcomes depending on imperviousness, soil type, terrain slope, and drainage infrastructure. The approach does not account for antecedent soil moisture conditions, snowmelt contributions, or compound rainfall–surge events. Accuracy is lower in regions with few or no quality-controlled hourly rain gauges, particularly in tropical and arid climates where extreme rainfall is highly localized.

2.1.2 Coastal Flooding

The coastal flood hazard layer provides probabilistic flood depth estimates for the 100-year return period at 1″ (∼30 m) resolution globally. The modeling framework combines three components of coastal water level:

1. **Astronomical tides.** Tidal water levels are derived from a global ocean tide model, providing high-frequency tidal variations at the coastline.
2. **Storm surge.** Extratropical storm surge is computed from multi-decadal atmospheric reanalysis fields. Tropical cyclone surge is computed from large synthetic tropical cyclone track sets (thousands of events per basin) that capture the full range of plausible storm intensities, tracks, and forward speeds. The combined surge climatology spans both tropical and extratropical forcing.
3. **Mean sea level.** A global mean dynamic topography correction ensures that modeled water levels are vertically consistent with the elevation data and accounts for spatial variations in mean sea level caused by ocean currents and density differences.

The resulting storm tide return levels are spatially interpolated along the coastline and used as boundary conditions for a connectivity-based inundation model. Water propagates inland from coastal seed pixels using a modified bathtub approach with distance-based energy attenuation. Attenuation rates vary by land cover type: lower attenuation in permanent waterways and tidal channels, higher attenuation over dry land and vegetated surfaces. Flood depth at each grid cell is computed as the difference between the propagated effective water level and the local terrain elevation.

Validation. Modeled storm tide return levels have been compared against tide gauge records with long observation histories at stations worldwide. Results are most reliable at stations with high-quality, multi-decadal records and

show larger departures where records are short or of mixed quality. Modeled inundation extents have been compared against satellite-observed flooding from major coastal storm events; agreement tends to be better in low-lying, open terrain and weaker in areas with natural barriers (dunes, ridges) or urban infrastructure that impedes flow but is not resolved in the DEM.

Strengths: Globally consistent; explicitly accounts for tropical cyclone surge via large synthetic event sets, not limited to the short historical record; high-resolution (∼30 m) coastal digital terrain model with spaceborne lidar correction provides substantially better vertical accuracy than standard satellite DEMs; probabilistic framework produces return-period estimates comparable to regulatory flood mapping standards.
Limitations: The inundation model is not mass, momentum, or energy conserving; inundation extents may be overestimated in areas where terrain features restrict flow. Does not account for wave runup—the additional vertical reach of water at the shoreline caused by breaking waves. Wave runup has two components: *setup*, a sustained rise in mean water level near shore due to the momentum of breaking waves, and *swash*, the oscillating rush of water up and down the beach face from individual waves. In exposed coastal settings, wave runup can add 1–3 m or more above the still-water storm tide level, meaning that assets near the shoreline may experience water contact even if they sit above the modeled flood elevation. Coastal flood protection infrastructure (seawalls, storm surge barriers, tide gates) is not represented in the hydraulic model (see Section 2.1.3 for defense overlay data). Compound flooding (simultaneous riverine discharge and elevated coastal water levels) is not captured. Coastal DEM vertical accuracy introduces meaningful uncertainty in very low-lying terrain where small elevation differences control inundation extent. Shoreline erosion, barrier island migration, and long-term geomorphological change are not modeled.

2.1.3 Flood Defense Data

Both the riverine and coastal flood hazard layers represent *undefended* flood hazard: levees, floodwalls, storm surge barriers, and other engineered defenses are not incorporated into the hydraulic or inundation models. This is a deliberate modeling choice—flood defense data is incomplete globally, defense condition and maintenance status are rarely documented, and defense failure during extreme events is a well-documented source of catastrophic loss.

To provide context on where flood defenses may reduce actual exposure, a global levee and coastal defense inventory has been compiled from official government sources and open-source infrastructure databases covering over 20 countries. The inventory is used as a spatial overlay to flag assets located in areas protected by engineered defenses.

Coverage and completeness:

- **Well-covered regions:** United States, Netherlands, United Kingdom, Germany, and Japan—where national levee registries or systematic infrastructure surveys exist.
- **Partially covered:** Much of Western Europe, South Korea, and selected river basins in South and Southeast Asia.
- **Limited or no coverage:** Sub-Saharan Africa, Central Asia, most of Latin America, and many island nations.

Where design heights are available, levees are assumed to provide protection up to their design capacity; elsewhere, only the presence of a defense structure is flagged without an assumed protection level. Users should note that the presence of a flood defense does not eliminate risk: defenses can be overtopped by events exceeding their design standard, can fail structurally, may degrade over time without adequate maintenance, and can lose effective freeboard due to land subsidence—a process that lowers both the defense crest and the land it protects relative to water levels, sometimes by several centimetres per year in deltaic and reclaimed-land settings.

2.2 Coastal Exposure

The Coastal Exposure Index identifies land areas whose elevation falls below hypothetical extreme coastal water level thresholds, providing a long-horizon screening tool for tidal and sea-level-rise exposure. It is not a probabilistic return-period product; unlike the coastal flood hazard layer (which estimates storm tide inundation depth at a specific return period), the Coastal Exposure Index answers a simpler but complementary question: *how close is this asset's elevation to current high water levels, and how much margin exists before chronic or permanent inundation becomes a concern?*

Because the index identifies low-lying coastal land irrespective of the cause of elevated water levels, it also provides useful screening context for other extreme coastal water level events that are not explicitly modeled elsewhere in this assessment, including tsunamis, seiches (resonant oscillations in enclosed or semi-enclosed water bodies such as harbors, bays, and lakes), and meteorological tides. Assets that sit close to or below the exposure threshold are inherently more vulnerable to any mechanism that raises coastal water levels, regardless of the specific forcing.

Methodology. The baseline water level is referenced to the mean higher high water (MHHW) tidal datum, which represents the average of the higher of the two daily high tides observed over a 19-year tidal epoch. Within the United States, MHHW is derived from published tidal benchmark stations maintained by the national tide gauge network. Outside the United States, MHHW is estimated from a global ocean tide model. Global mean dynamic topography corrections are applied to ensure vertical datum consistency between the tidal water levels and the elevation data.

Elevation data sources vary by region:

- **United States:** Lidar-derived digital elevation models at ∼1–3 m resolution, incorporating coastal defense structures (levees, seawalls) where mapped.
- **Global:** A satellite-corrected coastal digital terrain model at 1″ (∼30 m) resolution, consistent with the coastal flood hazard layer.

Areas are classified as exposed when land elevation falls below the selected water level threshold *and* is hydraulically connected to the coast. Topographically isolated low-lying areas (e.g. inland depressions below sea level that are not connected to tidal waters) are excluded by default using a connectivity-based algorithm.

Validation. The index has been compared against published national coastal exposure assessments. In lidar-covered areas, the exposed-area delineation shows close agreement with regulatory coastal flood zone boundaries. In satellite-DEM areas, the index captures the broad spatial pattern of coastal exposure, but individual asset classifications carry greater uncertainty due to the elevation accuracy limitations described above.

Strengths: Simple, transparent methodology that is easy to communicate to non-technical stakeholders; connectivity-based delineation avoids false positives from inland depressions; integrates coastal defense data within the United States; directly useful for screening sea-level-rise scenarios by adjusting the water level threshold (e.g. MHHW + 0.5 m, + 1.0 m); provides screening context for tsunami, seiche, and other extreme coastal water level events by identifying assets with limited elevation margin above current high water.
Limitations: Not based on physical storm or flood simulation; does not capture dynamic processes such as wave action, surge propagation, or flow routing. Does not account for shoreline erosion, barrier island migration, or long-term geomorphological change. Satellite-derived elevation accuracy introduces classification uncertainty for assets near the exposure threshold. Coastal defense data outside the United States is incomplete; the index may overstate exposure in well-defended areas. Best suited for long-term tidal and sea-level-rise screening; site-level decisions should be supported by local topographic surveys and coastal engineering assessment.

2.3 Temperature and Energy Demand

This section describes methods for assessing extreme temperature hazards and their contextual climate indicators. Heating and cooling demand layers differ from the other hazard layers in this product: they characterize climate-driven energy load rather than physical hazard, and are included as contextual indicators to support infrastructure sizing, operational planning, and energy cost screening.

2.3.1 Human Cold and Heat Stress

Extreme temperature hazards are assessed using a regionalization framework that combines station-level extreme value modeling with machine-learning-based spatial prediction. The analysis focuses on two metrics: (1) extreme cold temperature and (2) extreme wet-bulb temperature.

Quality-controlled weather station observations from global archives are used to fit extreme value distributions at each station. Wet-bulb temperature is calculated from daily air temperature and humidity observations. Annual block maxima (or minima for cold extremes) are modeled using a non-stationary generalized extreme value (GEV) framework that accounts for temporal trends, with return levels referenced to recent climatic conditions. Return levels are estimated for specified recurrence intervals (e.g., 10-year, 50-year).

To produce spatially continuous global fields at 30″ (∼1 km) resolution, station-derived distribution parameters are regionalized using a physics-informed machine learning model with high-resolution climate, elevation, and terrain predictors.

Advantages: Grounded in observed station data; non-stationary GEV framework quantifies uncertainty and references return levels to recent conditions; high-resolution (1 km) global estimates; explicitly models wet-bulb temperature for combined heat and humidity stress.
Limitations: Results depend on station density and record length. Wet-bulb calculations rely on humidity observation accuracy. The analysis characterizes meteorological extremes only and does not model vulnerability or infrastructure response.

2.3.2 Energy Demand

Heating and Cooling Degree Days (HDD and CDD) are provided as contextual climate indicators rather than hazard metrics. They are calculated from daily temperature fields derived from a high-resolution (30″; ∼1 km) global climate dataset for the period 2004–2023, produced using a statistical downscaling approach that accounts for topographic influences on temperature.

HDD and CDD are computed relative to a standard 18.3 °C (65 °F) balance-point temperature and aggregated to annual totals.

Advantages: High spatial resolution (1 km) with terrain-informed temperature fields; standardized methodology ensures cross-regional comparability.
Limitations: Degree-day metrics approximate temperature-driven demand only and do not account for humidity, solar gains, building efficiency, or behavioral adaptation. The fixed balance point may not represent all building types.

2.4 Snowfall Intensity

Snowfall intensity is assessed using a proxy derived from a global land-surface reanalysis product at ∼10 km resolution. Snowfall is estimated from positive day-to-day changes in snow depth (snow water equivalent, SWE) computed from daily mean snow depth fields spanning several decades of reanalysis record. For each year, the annual maximum 1-day SWE accumulation proxy is extracted, and the intensity metric is the long-term mean of these annual maxima, expressed in meters of SWE. **Advantages:** Multi-decadal record provides stable climatological estimates; global land coverage at ∼10 km resolution; consistent reanalysis-based methodology avoids reliance on sparse gauge networks for snowfall measurement.
Limitations: Snowfall is inferred from changes in snow depth rather than measured directly; the proxy underestimates true snowfall when within-day melt or compaction offsets accumulation. Conversion from SWE to physical snow depth requires an assumed snow density ratio. Reanalysis-based values in data-sparse regions carry greater uncertainty.

2.5 Wildfire

Estimating wildfire hazard is inherently complex due to the many interacting drivers of fire behavior, including atmospheric conditions, ignition sources, fuel availability, and fire suppression. All estimates should be carefully scrutinized.

The wildfire hazard model employs a physics-informed machine learning framework trained on high-fidelity wildfire simulation outputs covering the contiguous United States, Alaska, and Hawaii. The simulation-derived annual burn probability serves as the predictand. The predictor set comprises 23 features spanning fire weather climatology, atmospheric moisture demand, precipitation regime, vegetation and fuel structure, terrain, and ignition proxies.

Training samples ($n \approx 3.1 \times 10^6$) are drawn from the conterminous United States, Alaska, and Hawaii using geographic stratification. Model evaluation uses five-fold spatial block cross-validation with 0.5° geographic blocks, yielding $R^2 = 0.83 \pm 0.01$ in log-transformed space. Global inference is performed at 10″ (∼300 m) resolution, with predictions masked to burnable land classes. Wildland–urban interface (WUI) regions are identified from land use/land cover data as urban areas neighboring large vegetated areas; burn probability scores for these zones are derived from the surrounding vegetated landscape to reflect the realistic ignition exposure faced by assets at the urban–wildland boundary.

Advantages: High-resolution (300 m) global coverage for screening purposes; physically motivated predictor set spanning fire weather, fuel, terrain, and ignition; spatial cross-validation demonstrates geographic robustness within the training domain. Because this is a proprietary model without a published external reference, additional methodological detail is provided in the full (unabbreviated) version of this document. Results outside the U.S. training domain should be treated as indicative of fire-prone conditions rather than calibrated burn probability estimates.

Limitations: The model is trained exclusively on U.S. burn probability data; transferability to other continents has not been formally validated. Tropical savanna and peatland fire regimes are not represented in the training data. The framework does not explicitly simulate ignition frequency, human suppression, or dynamic fire spread.

2.6 Drought

Meteorological drought is assessed using basin-scale precipitation deficits derived from observation-constrained reanalysis data. Precipitation drought metrics are computed at two complementary spatial scales: hydrologically defined watersheds and first-order administrative regions for complete global coverage.

Long-term daily precipitation from a global reanalysis product is aggregated to multi-year accumulations to capture persistence relevant to water supply systems and reservoir storage. Extreme value analysis is applied to annual minima of rolling multi-year precipitation accumulations to estimate return levels for rare drought events (e.g., 25-year, 50-year, 100-year).

The composite drought hazard score (0–100) emphasizes absolute hydrological scarcity rather than relative departures from local climatology. For each spatial unit, remaining water is estimated as the climatological mean precipitation minus the rare drought deficit. This quantity is then transformed into a globally comparable score using a percentile-based ranking, where regions with the least remaining water receive the highest scores.

Advantages: Emphasizes physical water availability rather than statistical anomaly magnitude; enables consistent comparison across wet and dry climates; aligns with infrastructure planning horizons through use of rare drought.
Limitations: Reflects meteorological water availability only; does not incorporate groundwater storage, reservoir operations, interbasin transfers, or water demand. Spatial aggregation smooths local variability. Reanalysis-based precipitation carries uncertainty in data-sparse regions.

2.7 Wind and Convective Storms

This section describes methods for assessing hazards related to extreme wind and convective storm activity, including tropical cyclone winds, thunderstorm frequency, large hail, and tornadoes.

2.7.1 Extreme Wind

Annual maximum 3-second wind gust estimates are produced at 30″ (∼1 km) over land and nearshore regions. Gusts capture both tropical-cyclone (TC) and non-TC drivers. TC wind fields are derived from synthetic tropical cyclone track datasets, converted to 3-second gusts via a gust factor, and adjusted for surface roughness using satellite-derived land cover data. Non-TC gusts are estimated from reanalysis data using a parametric gust profile methodology calibrated against in situ observations. The two components are combined by taking the maximum of the TC and non-TC return-level estimates at each grid cell, ensuring that the dominant wind hazard source is represented regardless of location. The approach provides smooth fields in flat terrain and resolves fine-scale variability in mountainous regions.

Advantages: Downscaling procedure improves local reanalysis gust estimates; combines TC and non-TC wind hazard in a single layer.
Limitations: Highly localized phenomena (downbursts, derechos, tornadic winds) are not captured. The non-TC gust regression is calibrated against European observations only; transferability to other regions has not been independently validated.

2.7.2 Thunderstorm Frequency

Global thunderstorm frequency is assessed using a satellite-calibrated lightning detection dataset. Thunderstorm occurrence is represented using the *thunder hour* metric: any one-hour period with at least two lightning strokes detected within a specified radius of a location is counted as a thunder hour. These data are aggregated to annual totals on a uniform global grid at ∼5 km resolution.

Advantages: Near-global coverage and consistent thresholds enable cross-region comparability; multi-year records emphasize robust spatial patterns.
Limitations: Detection efficiency varies by region and stroke intensity; using lightning as a proxy for thunder audibility introduces uncertainty.

2.7.3 Large Hail

The large hail layer is based on a global climatology of very large hail (VLH; ≥ 5 cm / 2 in), derived from a statistical convective hazard model applied to atmospheric reanalysis data at ∼31 km resolution over a multi-decadal period. The model estimates the probability of VLH occurrence at each grid point by combining the probability of thunderstorm occurrence with the conditional probability of VLH given a thunderstorm. Atmospheric predictors include measures of instability, vertical wind shear, moisture, and other convective parameters.

Advantages: Multi-decadal globally consistent climatology derived from physically interpretable environmental predictors; reproduces known regional hotspots and seasonal cycles.
Limitations: Reanalysis data do not explicitly simulate hail; VLH occurrence is inferred from environmental conditions via a statistical model. Model skill may vary in regions with sparse observational records.

2.7.4 Tornadoes

The tornado layer provides a U.S. climatology of significant tornado activity (EF2+), derived from historical tornado records. The metric represents the annual probability of an EF2+ tornado occurring within a specified radius of a given location, calculated over a multi-decadal baseline period. EF2+ tornadoes are the focus because they are associated with substantial structural damage and are more consistently reported over time.

Advantages: Observationally based with standardized EF-scale ratings; spatial aggregation produces a stable screening metric.
Limitations: Tornado records are influenced by reporting practices, radar deployment, and population density. The dataset reflects historical frequency only and does not account for future climate change.

2.7.5 Derechos

Derechos are long-lived, widespread convective windstorms produced by organized mesoscale convective systems, typically associated with bow echoes. They are characterized by persistent swaths of damaging straight-line winds extending over hundreds of kilometres and pose significant threats to utility infrastructure, forestry, agriculture, and the built environment.

The derecho hazard layer is derived from a peer-reviewed observational derecho climatology covering the United States east of the Rocky Mountains over an 18-year period. The dataset was constructed using an automated

detection framework that integrates satellite-based storm tracking, machine-learning bow-echo identification, and physically based derecho classification criteria, at 4 km spatial resolution.

Event footprints are converted to binary masks and summed across all events, then divided by the number of years to produce an annualized derecho-footprint frequency field (yr^{-1}). The raw field is spatially smoothed using a moving-window mean to produce a generalized climatological hazard surface suitable for regional screening.

Advantages: Based on a peer-reviewed observational dataset with physically based event-identification criteria; high spatial resolution (4 km); annualized frequency metric is intuitive and directly comparable across locations.
Limitations: Coverage is limited to the United States east of the Rocky Mountains. The 18-year record may not fully capture long-term frequency of rare events. Spatial smoothing generalizes native-resolution footprint edges.

2.8 Geohazards

2.8.1 Seismic Hazard

The seismic hazard layer represents peak ground acceleration (PGA) with a 10% probability of exceedance in 50 years (return period of 475 years), expressed in units of g. It is compiled as a global approximately 1 km resolution raster by merging the best available regional probabilistic seismic hazard models with a global background layer. Over 20 regional models are incorporated, covering the United States, Canada, Europe, the Middle East, South America, Southeast Asia, Australia, New Zealand, and other regions. Where regional models exist, they take precedence over the global background. All models assume rock or firm-rock site conditions.

Advantages: Globally consistent estimates aligned with engineering standards; reference rock conditions ensure comparability; merges best available regional models with global coverage.
Limitations: All values assume rock or firm-rock site conditions; actual ground shaking at a specific site can differ materially in soft-soil basins, fill, or liquefiable deposits where site amplification may substantially increase PGA. Secondary hazards (liquefaction, surface rupture, tsunamis) are not represented. Boundary discontinuities may exist between mosaicked regions.

2.8.2 Landslides

For regions outside the United States, landslide hazard is assessed using a global rainfall-driven model that combines terrain susceptibility (based on slope, lithology, vegetation, and soil moisture) with extreme rainfall data to estimate the conditional probability of landslide initiation at 3″ ($\sim$90 m) resolution.

Within the United States, landslide susceptibility is assessed using terrain-based threshold models trained on a national compilation of documented landslides and high-resolution digital elevation data. Model outputs are provided at 90 m resolution.

Because the U.S. and global products are derived from different underlying models, they should be interpreted as separate screening layers rather than directly comparable indices.

Advantages: Global framework integrates rainfall forcing and terrain susceptibility at high resolution; U.S. models are empirically calibrated against a comprehensive landslide inventory.
Limitations: Global rainfall forcing data are coarse and may miss localized extremes. U.S. models are terrain-based and do not incorporate dynamic rainfall triggering; they represent relative susceptibility rather than event probability.

2.8.3 Land Subsidence

Land subsidence refers to the vertical sinking of the land surface. Subsidence estimates are derived from a global physics-informed machine learning model trained on quality-controlled observation points, using predictors including groundwater abstraction, climate, geology, and topography. The resulting dataset is provided at 30″ ($\sim$1 km) resolution.

Advantages: Globally consistent 1 km estimates; diverse predictors capture key physical drivers of subsidence.
Limitations: The model predicts subsidence rates from environmental covariates; it does not assimilate direct observations at every location, and localized anthropogenic drivers—particularly intensive groundwater extraction, underground mining, and hydrocarbon withdrawal—can dominate subsidence rates in ways that global predictors do not fully resolve. Local-scale rates can therefore differ substantially from gridded estimates. The model represents near-present-day conditions and does not project future changes.

3 Hazard Rating Scale

Each hazard layer in the Hazard Explorer is assigned an integer rating from 0 (negligible or below detection) to 10 (extreme). Ratings provide a standardized basis for comparing relative hazard severity across layers and locations.

Score bin boundaries are set using expert judgment informed by the global empirical distribution of each metric, known engineering relevance thresholds where applicable, and the goal of maintaining interpretability across the 1–10 scale. Thresholds are chosen to distribute scores broadly: a score of 5 should represent meaningfully greater exposure than a score of 2, and the highest scores are generally reserved for values that are rare in the global distribution or that exceed meaningful engineering relevance thresholds. Some layers exclude zero or near-zero values before setting bins to avoid compressing the active range (e.g., heating and cooling demand, hazards with large areas of zero exposure).

Human Cold Stress scores are inverted: lower (more extreme) temperatures correspond to higher scores. The global landslide layer uses a fixed categorical mapping from raw susceptibility classes to hazard scores (see table footnote).

Table 3 shows the minimum metric value required for each hazard rating. Values below the score 1 threshold receive a rating of 0.

Table 3: Hazard rating scale: minimum metric value for each score level.

Hazard Layer	Unit	1	2	3	4	5	6	7	8	9	10
Wildfire	%/yr	0.05	0.15	0.25	0.35	0.50	0.70	1.00	1.50	2.50	4.00
Extreme Heat	°C	25	31	34	36	38	40	42	44	47	51
Human Heat Stress	°C	16.0	21.0	23.0	25.0	27.0	28.5	29.5	30.5	31.5	33.0
Human Cold Stress†	°C	14.0	8.1	1.4	−3.3	−10.1	−24.7	−34.2	−42.2	−46.5	−49.9
Drought	score	0	27	37	44	51	60	62	71	83	91
Flood Depth (100-yr)	m	0.01	0.05	0.10	0.25	0.50	0.75	1.00	1.50	2.00	3.00
Surface Water Flooding	mm	0	15.2	18.0	21.8	28.3	40.5	53.7	74.7	104.6	121.7
Extreme Wind	km/h	68	85	100	115	130	145	165	185	210	250
Lightning	hr/yr	1	5	10	20	40	60	80	120	180	300
Large Hail	%/yr	0.01	0.3	1.0	2.0	3.0	3.9	7.7	13.9	22.1	33.0
Tornado (EF2+)	%/yr	0.1	0.5	1.5	3.0	6.0	10.0	14.0	18.0	25.0	35.0
Derecho (U.S.)	events/yr	0.05	0.09	0.15	0.25	0.39	0.62	1.01	1.56	2.23	3.00
Earthquake	g	0.01	0.02	0.03	0.05	0.08	0.10	0.20	0.30	0.40	0.50
Land Subsidence	mm/yr	1.5	2	3	4	5	7	10	15	25	50
Landslide (U.S.)	index (0–81)	0	0	1	3	6	12	20	32	46	60
Landslide (Global)‡	class (0–5)	Fixed mapping: raw class 2 → 4; 3 → 7; 4 → 8; 5 → 10. Raw class ≤ 1 = no hazard.									
Heating Demand	°C-day	61	344	853	1 800	3 012	4 098	5 214	6 396	8 393	10 700
Cooling Demand	°C-day	18	84	280	658	1 156	1 771	2 349	2 749	3 010	3 267

† Inverted: lower temperatures correspond to higher scores.
‡ Uses a fixed categorical mapping rather than threshold bins.

4 General Limitations and Considerations

The following limitations apply to all hazard layers and should be considered when interpreting results for any specific application.

1. **Hazard Is Not Risk.** These layers characterize physical hazard and hazard exposure, not asset-specific risk. They do not account for vulnerability, fragility, replacement cost, occupancy, downtime consequences, construction type, or existing mitigation measures unless explicitly noted. Two assets with identical hazard scores may face very different financial or operational consequences depending on their construction, use, and resilience measures. Risk quantification requires additional inputs beyond what is provided here.
2. **Scope: Screening, Not Assessment.** The Hazard Explorer is designed for first-stage triage of large portfolios. Its outputs identify assets warranting further investigation; they are not loss estimates, engineering findings, or regulatory determinations. A high score should trigger follow-on site-specific study by a qualified engineer or hazard specialist before any investment or design decision is made. A low score provides screening-level assurance that hazard exposure does not appear elevated relative to global baselines—it does not certify that a site is free of hazard.
3. **False Negatives vs. False Positives.** Because this tool is designed to cast a wide net, conservative scoring thresholds and overlapping hazard layers are used to minimize the risk of missing genuinely high-risk assets. Some assets will be flagged that, upon closer inspection, do not warrant further investigation—this is an acceptable outcome of screening. Users should not interpret the absence of a flag as definitive clearance, particularly for localized or highly site-specific hazards such as convective storms, flash flooding, or slope instability.
4. **Resolution and Modeling Limitations.** All hazard layers involve simplifying assumptions, including limited spatial resolution, imperfect observational records, and parametric modeling choices. Results are especially sensitive to these limitations for localized hazards and in data-sparse regions. Users should incorporate multiple lines of evidence—including observed historical events, local knowledge, and alternative datasets—before drawing conclusions about any single location.
5. **Temporal Validity.** The data and methods reflect conditions at the time of publication. Climate-driven hazards in particular are subject to non-stationarity; return levels calibrated on historical records may understate future risk. Results should be revisited as observational records lengthen and methods improve.

5 Data Sources and Licensing

The hazard layers in this product draw on a wide range of third-party datasets, including global reanalysis products, satellite-derived climatologies, weather station observations, digital elevation models, tidal databases, land cover classifications, and published hazard models. All layers also incorporate proprietary methodologies developed by Degree Day, LLC. Table 4 summarises the relevant third-party data licences for each hazard layer.

Table 4: Third-party data licences by hazard layer.

Hazard Layer	Third-Party Data Licences
Wildfire	CC BY 4.0
Extreme Heat	Public domain; CC0
Human Heat Stress	Public domain; CC0
Human Cold Stress	Public domain; CC0
Snowfall Intensity	CC BY 4.0
Heating Demand	CC0
Cooling Demand	CC0
Drought	CC BY 4.0
Riverine Flood	CC BY 4.0; Copernicus licence
Coastal Flood	CC BY 4.0; Copernicus licence
Coastal Exposure	CC BY 4.0; Public domain
Surface Water Flooding	CC BY 4.0; Public domain
Extreme Wind	CC BY 4.0
Lightning	CC BY-SA 4.0
Large Hail	CC BY 4.0
Tornado (U.S.)	Public domain
Derecho (U.S.)	CC BY 4.0
Earthquake	Public domain; CC BY-SA 4.0
Landslide (U.S.)	Public domain
Landslide (Global)	CC BY 4.0
Land Subsidence	CC BY 4.0

A detailed inventory of all datasets, providers, and licence terms is available in the full (unabbreviated) version of this methodology document.

Degree Day

www.degreeday.org

info@degreeday.org